Double-energy-differential cross sections for the Coulomb four-body problem in a quasiclassical framework

Agapi Emmanouilidou
ITS, University of Oregon, Eugene, Oregon 97403-5203, USA
(Received 28 January 2007; published 11 April 2007)

In a quasiclassical framework, we formulate the double-energy-differential cross sections for the Coulomb four-body problem. We present results for the triple photoionization from the Li ground state at 115, 50, and 3.8 eV excess energies. With the energy of one of the electrons kept fixed, the double-energy-differential cross sections at 115 eV excess energy is found to be of "U-shape" (unequal energy sharing), and in very good agreement with *ab initio* results. At 50 eV, it seems that a transition starts taking place to more equal energy sharing configurations. Close to threshold, at 3.8 eV excess energy, the equal energy sharing configurations are the dominant ones.

DOI: 10.1103/PhysRevA.75.042702 PACS number(s): 32.80.Fb, 03.65.Sq

I. INTRODUCTION

Several theoretical approaches and experimental results, in good agreement with each other, are available for the single photon double ionization of the helium atom (Coulomb three-body problem) [1]. At the same time the single photon triple ionization of the lithium atom (Coulomb four-body problem) is still largely unexplored.

Regarding the total triple photoionization cross section from the ground state of Li the few existing theoretical results [2–4] are in good agreement with experiment [5,6]. However, for differential cross sections of three escaping electrons the theoretical studies are very limited with no experimental results currently available. The small number of theoretical studies and the current lack of experimental ones is partly due to the very small values of the differential cross sections. With the highest value of the total triple photoionization cross section for Li being a few barns, the differential ones are even smaller since they sample only part of the outgoing flux. However, there are recent experimental results for differential cross sections of three outgoing electrons for the electron-impact double ionization of helium. These experiments measure the angular distribution of two ionized electrons when the incoming electron is very fast [7–9] and more recently measurements were obtained for incident electrons of much lower energy [10]. The theoretical work on differential cross sections for triple photoionization from the Li ground state include: (a) A study of selection rules for different electron-momenta configurations in the three electron escape [11]. In this work, various relative angular distributions of one of the outgoing electrons (for a given relative angle of the other two electrons) were presented using correlated 6 C (Coulomb) final state wave functions. (b) There is also a very recent study of energy-differential cross sections for photon energies of 280, 300, and 320 eV for the triple photoionization of Li using the nonperturbative time-dependent close coupling method [12]. (c) Finally, in Ref. [13] the angular correlation probability is evaluated in the framework of classical mechanics. The angular correlation depends only on the relative angle between any pair of ionized electrons in the three electron escape.

In the current paper, we investigate double-energy-differential cross sections for the triple photoionization from the Li ground state. To our knowledge, it is the first time double-energy differential cross sections are formulated classically. Energy differential cross sections for the complete break-up of the Li atom are much more difficult to interpret compared to those for the complete break-up of the He atom. For two electron escape, for a given excess energy, there is only one energy-differential cross section as a function of one electron's energy. For three electron escape, for a given excess energy, a different double-energy-differential cross section, as a function of one electron's energy, is obtained for each energy assigned to one of the electrons (see below slices through differential cross sections). Our results are obtained using a quasiclassical formulation which has been outlined elsewhere [4] but we include it here as well, in Sec. II A, for completeness of the paper. The classical nature of our investigation results in three distinguishable escaping electrons. In Sec. II B, we outline how starting from the double-energy differential cross sections of the three distinguishable electrons we obtain fully symmetrized ones. Note that, in an *ab initio* formulation the symmetry properties of the differential cross section are a natural outcome of using a fully antisymmetric wave function to describe the three electron state. In Sec. II C, we discuss how the double-energy differential cross sections are computed numerically. In Sec. III, we present the double-energy differential cross sections for three different excess energies: for 115, 50, and 3.8 eV. For the case of 115 eV we directly compare our results with the *ab initio* double-energy differential cross sections in Ref. [12] for a photon energy of 320 eV.

II. QUASICLASSICAL FORMULATION OF SINGLE PHOTON MULTIPLE IONIZATION

A. Initial phase space density and its time evolution for single photon triple ionization

The construction of the initial phase space density $\rho(\gamma)$ in our quasiclassical formulation of the triple photoionization of Li has been detailed in [4], here we give only a brief summary. We formulate the triple photoionization process from the Li ground state ($1s^2 2s$) as a two step process. First, one electron absorbs the photon (photoelectron) at time $t=t_{\mathrm{abs}}$

=0. Through electronic correlations, the energy gets redistributed, resulting in three electrons escaping to the continuum. We express the above two step process as

$$\sigma^{3+} = \sigma_{\mathrm{abs}} P^{3+}, \tag{1}$$

where σ_{abs} is the total absorption cross section and P^{3+} is the probability for triple ionization. In what follows, we use the experimental data of Wehlitz [6] for σ_{abs}. Our formulation accounts for the second step. We first assume that the photon is absorbed by a $1s$ electron at the nucleus ($\mathbf{r}_1=0$). This latter approximation becomes exact in the limit of high photon energy [14]. The cross section for photon absorption from a $1s$ orbital is much larger than from a $2s$ orbital [15]. Hence, we can safely assume that the photoelectron is a $1s$ electron which significantly reduces the initial phase space to be sampled. Also, by virtue of their different character the electrons become practically distinguishable and allow us to neglect antisymmetrization of the initial state. We denote the photoelectron by 1, the other $1s$ electron by 2, and the $2s$ electron by 3. Following photon absorption, we model the initial phase space distribution of the remaining two electrons, $1s$ and $2s$, by the Wigner transform of the corresponding initial wave function $\psi(\mathbf{r}_1=0,\mathbf{r}_2,\mathbf{r}_3)$, where $\mathbf{r}_i$ are the electron vectors starting at the nucleus. We approximate the initial wave function as a simple product of hydrogenic orbitals $\phi_i^{Z_i}(\mathbf{r}_i)$ with effective charges Z_i, to facilitate the Wigner transformation. The Z_i are chosen so that they reproduce the known ionization potentials I_i, namely for the 2s electron $Z_3=1.259$ ($I_3=0.198$ a.u.) and for the $1s$ electron $Z_2=2.358$ ($I_2=2.780$ a.u.). (We use atomic units throughout the paper if not stated otherwise.) The excess energy, E, is given by $E=E_\omega-I$ with E_ω the photon energy and $I=7.478$ a.u. the Li triple ionization threshold energy. Given the above considerations, the initial phase space density is given by

$$\rho(\gamma) = \mathcal{N}\delta(\mathbf{r}_1)\,\delta(E_1+I_1-\omega)\prod_{i=2,3} W_{\phi_i^{Z_i}}(\mathbf{r}_i,\mathbf{p}_i)\,\delta(E_i+I_i) \tag{2}$$

with normalization constant $\mathcal{N}$.

We next determine which fraction of $\rho(\gamma)$ leads to triple ionization, by following the phase space distribution in time. The evolution of a classical phase space density is determined by the classical Liouville equation

$$\frac{\partial \rho(\Gamma(t))}{\partial t} = \mathcal{L}_{\mathrm{cl}}\rho(\Gamma(t)), \tag{3}$$

with the initial phase space values being

$$\Gamma(0) \equiv \gamma, \tag{4}$$

and $\mathcal{L}_{\mathrm{cl}}$ the classical Liouville operator which is defined by the Poisson bracket $\{H,\}$, with H the Hamiltonian of the system. In our case H is the full Coulomb four-body Hamiltonian. We determine the triple ionization probability P^{3+} formally through

$$P^{3+} = \lim_{t\to\infty}\int_{t_{\mathrm{abs}}}^{t} d\Gamma_{\mathcal{P}^{3+}} \exp[(t-t_{\mathrm{abs}})\mathcal{L}_{\mathrm{cl}}]\rho(\Gamma). \tag{5}$$

The projector $\mathcal{P}^{3+}$ indicates that we integrate only over those parts of phase space that lead to triple ionization. In practice, Eq. (5) amounts to discretizing the initial phase space, assigning weights to each discrete point $\gamma_j=(p_j(0),q_j(0))$ according to $\rho(\gamma_j)$, and evolving in time each initial condition γ_j with the Coulomb four-body Hamiltonian. We propagate the electron trajectories using the classical equations of motion (classical trajectory Monte Carlo method [16,17]). Regularized coordinates [18] are used to avoid problems with electron trajectories starting at the nucleus. We label as triple ionizing those trajectories where the energies off all three electrons are positive, $E_i>0$ with $i=1,2,3$, asymptotically in time. We evaluate P^{3+} by adding the weights of all triply ionized trajectories.

B. Double differential probabilities

Our goal is to formulate the double-energy-differential cross section $d^2\sigma^{3+}/dE_\alpha dE_\beta$. It should be such that when doubly integrating over it the total triple ionization cross section is recovered,

$$\sigma^{3+} = \int_0^E dE_\alpha \int_0^{E-E_\alpha} dE_\beta \frac{d^2\sigma^{3+}}{dE_\alpha dE_\beta} \equiv \sigma_{\mathrm{abs}}\int_0^E dE_\alpha \int_0^{E-E_\alpha} dE_\beta \frac{d^2P^{3+}}{dE_\alpha dE_\beta}. \tag{6}$$

In what follows, we formulate $d^2P^{3+}/dE_\alpha dE_\beta$.

As it has already been mentioned in Sec. II A, by considering a product of hydrogenic orbitals as our initial state, we neglect antisymmetrization in the initial state. The three escaping electrons are distinguishable resulting in three distinct double differential probabilities $d^2P^{3+}(E_i,E_j)/dE_i dE_j$ with the energy of the third electron being $E_k=E-E_i-E_j$ from conservation of energy and $i,j,k=1,2,3$, $i<j$. We next symmetrize each one of the above three double differential probabilities as follows: $d^2P^{3+}(E_i,E_j)/dE_i dE_j$ should be (a) symmetric under exchange of the electron indices, that is, it should have the same value when $E_i\to E_j$ since electrons i and j are indistinguishable; (b) for constant energy E_i the double differential probability, which is now only a function of E_j, should be symmetric with respect to $(E-E_i)/2$ since electrons j and k are indistinguishable; for constant energy E_j the double differential probability, which is now only a function of E_i, should be symmetric with respect to $(E-E_j)/2$ since electrons i and k are indistinguishable; the double differential probability that satisfies the above properties is of the following form:

$$\frac{d^2P^{3+}_{\mathrm{sym}}(E_i,E_j)}{dE_i dE_j} = \frac{1}{6}\left(\frac{d^2P^{3+}(E_i,E_j)}{dE_i dE_j} + \frac{d^2P^{3+}(E_j,E_i)}{dE_i dE_j} + \frac{d^2P^{3+}(E_i,E-E_i-E_j)}{dE_i dE_j} + \frac{d^2P^{3+}(E-E_i-E_j,E_i)}{dE_i dE_j}\right.$$

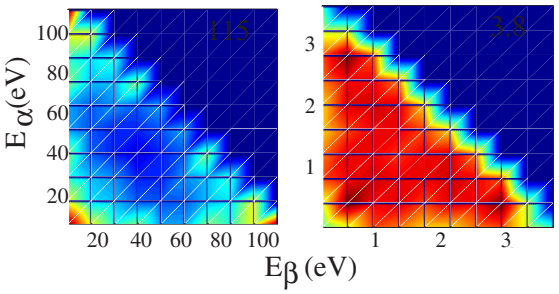

FIG. 1. (Color online) Contour plots of the double-energy-differential cross section for excess energies 115 and 3.8 eV. The trianglelike structure close to the $E_\alpha = E - E_\beta$ line is an artifact of our choice of square bins.

$$+\frac{d^2P^{3+}(E_j,E-E_i-E_j)}{dE_i dE_j}$$

$$+\frac{d^2P^{3+}(E-E_i-E_j,E_j)}{dE_i dE_j}\Bigg). \tag{7}$$

It now follows that the symmetrized double differential probability is given by

$$\frac{d^2P^{3+}(E_\alpha,E_\beta)}{dE_\alpha dE_\beta} = \sum_{i<j}\frac{1}{3}\left(\frac{d^2P^{3+}_{\rm sym}(E_i,E_j)}{dE_i dE_j}\right), \tag{8}$$

where the normalization factor follows from

$$\int_0^E dE_\alpha \int_0^{E-E_\alpha} dE_\beta \frac{d^2P^{3+}(E_\alpha,E_\beta)}{dE_\alpha dE_\beta} = P^{3+}. \tag{9}$$

C. Numerical evaluation of double differential probabilities

To numerically evaluate the three $dP^{3+}(E_i,E_j)/dE_i dE_j$ we divide the energy surface $[0,E][0,E]$ into N^2 equally sized square bins. We then find the triple ionized trajectories which fall into the bins and add up their weights. Note that from conservation of energy the double-energy-differential probabilities map out a triangle, see Sec. III. The size of N is chosen so that we have a small standard relative error for each square bin (the error is inversely proportional to the square root of the number of triple ionizing events in a given square bin [16]). For each of the excess energies currently under investigation the number of triple ionizing trajectories used in our computations was no less than 8000.

III. RESULTS

In this section we present results for excess energies of 115, 50, and 3.8 eV. Our choice of excess energies allows us to investigate the double differential cross sections for energies close to threshold (3.8 eV), close to the energy where the total cross section is maximum (50 eV) and for higher energies (115 eV). Note, that the 115 eV is in the energy range where our quasiclassical formulation is still valid (for very high excess energies one must treat the problem quantum mechanically). In Fig. 1 we plot the double-energy-differential cross section for two excess energies, namely 115 and 3.8 eV, to illustrate the difference in energy sharing of the three escaping electrons at large (115 eV) and small (3.8 eV) excess energies. The figure clearly illustrates that the double differential cross section has the symmetries discussed in Sec. II B. In addition, one can see that at large excess energies, 115 eV, the differential cross section has a bowl shape. That is, for a given energy of one of the electrons the other two electrons share unequally the remaining energy, see below. On the other hand, at 3.8 eV for a given energy of one of the electrons the other two electrons tend to roughly equally share the remaining energy.

To gain more insight into the double differential cross sections, we consider in Figs. 2–4 slices through the double-energy-differential cross sections for each of the four excess energies. That is, fixing the energy of one of the three escaping electrons, E_α, we plot the double differential cross section as a function of the energy of another escaping electron, E_β. The energy of the third outgoing electron can be found from conservation of energy. For all excess energies considered the energy surface $[0,E][0,E]$ is binned in N^2 squares with $N=14$ for 115 and 50 eV while $N=10$ for 3.8 eV.

In addition, for excess energy of 115 we see that the slices through the double differential cross section have a "U-shape." The latter is the well-known characteristic shape of the single-energy-differential cross section for two outgoing electrons for high photon energies. In Ref. [12], the slices through the differential cross sections were all found to be of "U-shape." We next compare our quasicalssical results with the *ab initio* results of Ref. [12] for 320 eV photon energy. The comparison is only an approximate one since our binning restricts the energies E_α we can consider. The value of E_α we use to compare is the one closer to the energy considered by the quantum calculations. Also note that the photon energy of 320 eV corresponds to a slightly higher excess energy than the 115 eV excess energy favoring a shape of

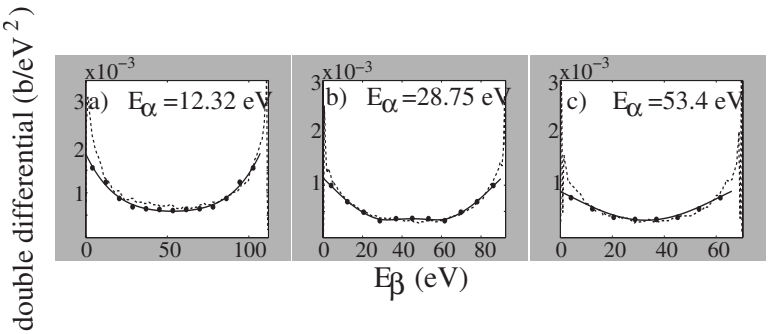

FIG. 2. Double-energy-differential cross section for $E=115$ eV. The cross section is shown as a function of one electron's energy when the energy of one of the electrons is fixed to 12.32 eV, 28.75 eV, and 53.4 eV. Dashed black lines are the data extracted from Ref. [12] for a 320 eV photon energy.

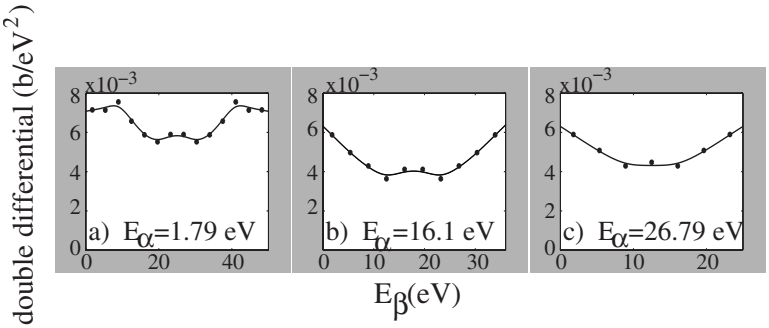

FIG. 3. Double-energy-differential cross section for $E=50$ eV. The cross section is shown as a function of one electron's energy when the energy of one of the electrons is fixed to 1.79 eV, 16.1 eV, and 26.79 eV.

slightly more unequal energy sharing than the ones considered in Figs. 2(a)–2(c). We compare our results for 12.32, 28.75, 53.4 eV, respectively, with the results of Ref. [12] for 10, 30, 50 eV (dashed line) in Figs. 2(a)–2(c). Our data points are the black circles while the solid lines are a fit to these data points (the same holds for Figs. 3 and 4. We find that our results for 115 eV excess energy compare very well with those of Ref. [12]. The agreement is very good for intermediate values of E_β while it is not as good close to the edges. However, close to the edges, as the authors in Ref. [12] point out, their results are less accurate due to some lack of convergence. From Fig. 2 we see that for large excess energies the smaller E_a is the more pronounced the unequal energy sharing between the two electrons is. That means that for a very small energy of one electron a highly unequal energy sharing is favored among the other two. For a very large energy of one electron the unequal energy sharing of the other two is not as pronounced.

We next focus on the slices through the double differential cross sections for excess energies of 50 and 3.8 eV, with the latter being very close to threshold, see Figs. 3 and 4. One notices that at 50 eV for $E_a=1.79$ eV [see Fig. 3(a)] the maximum of the differential cross section shifts to an energy $E_\beta \neq 0$ unlike the 115 eV excess energy where the maximum is at $E_\beta=0$. In addition, one sees from Fig. 3 that equal energy sharing among two of the electrons is favored for intermediate E_β energies (hump in the middle of the E_β energy range). It thus, seems, that at 50 eV excess energy a transition starts taking place from a highly unequal energy sharing at 115 eV to a more equal one. At 3.8 eV, an energy very close to threshold, the transition to equal energy sharing configurations becomes even more pronounced. A comparison of Figs. 3 and 4 shows that the maximum of the differential cross section for 3.8 eV has shifted to energies E_β higher than those for 50 eV and for $E_\alpha=1.71$ eV, see Fig. 4(c)), equal energy sharing is the favorable configuration. What is also quite interesting is that at 3.8 eV the slices through the double differential cross sections as the energy E_α is increased, see Figs. 4(a)–4(c), have shapes similar to those of the single-energy-differential cross sections of the two electron escape for decreasing excess energy close to threshold, see, for example, [19].

It is clear that a thorough study of the slices through the double-energy differentials for the three electron escape is needed for a large number of excess energies. Such a study can answer the question of how the transition takes place from a "U-shape" at higher excess energies (115 eV) to more equal energy sharing for energies closer to the energy of the maximum of the triple ionization cross section (50 eV), and finally to energies where equal energy sharing is the favorable configuration (3.8 eV). Understanding how the transition takes place will ultimately help us understand how the behavior of the three escaping electrons changes with decreasing excess energy. To compare with two electron escape, let us point out that in the latter case a transition of the single-energy-differential cross section takes place from an unequal energy sharing to an equal sharing one as the photon energy decreases. For the case of He double ionization, at 100 eV photon energy (close to the energy where the maximum of the double ionization cross section is) the single-energy-differential cross section is flat. 100 eV is the critical energy where the transition from unequal to equal energy sharing starts taking place for two electron escape [20,21]. In addition, for the case of electron-hydrogen scattering [19], as the excess energy is decreased (for energies close to threshold) it was found that the single differential cross sections have shapes similar to those shown in Fig. 4. What are the physical implications of this similarity for the three electron case remains to be seen.

IV. CONLUSIONS

We have presented the quasiclassical study of double-energy-differential cross sections for the triple ionization of

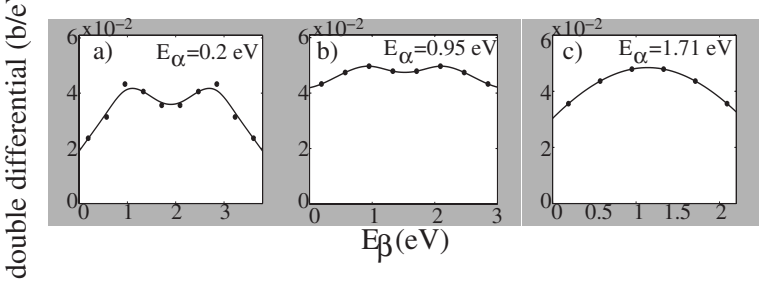

FIG. 4. Double-energy-differential cross section for $E=3.8$ eV. The cross section is shown as a function of one electron's energy when the energy of one of the electrons is fixed to 0.2 eV, 0.95 eV, and 1.71 eV.

the lithium ground state. For 115 eV our results are in very good agreement with the *ab initio* double-energy-differential cross sections in Ref. [12] for a photon energy of 320 eV. This agreement indicates that our simple initial state of a product wave function correctly captures the essential features of the triple ionization process by single photon absorption from the Li ground state. At 50 eV, it seems that a transition starts taking place from a "U-shape" to a more equal energy sharing configuration. We find that at 3.8 eV the slices through the double-energy-differential cross section have transitioned roughly to shapes where equal energy sharing is favored. We believe that our first results on how the transition towards threshold takes place will be the impetus for future studies of double-energy-differential cross sections as the excess energy is reduced down to threshold. It could be the case that these detailed studies for a large number of excess energies will allow a connection between the shapes of the double-energy-differential cross sections and the sequences of collisions that the three electrons follow to escape [13].

ACKNOWLEDGMENT

The author is indebted to Y. Smaragdakis, J. M. Rost, and T. Pattard for discussions and for a critical reading of this paper.

[1] J. S. Briggs and V. Schmidt, J. Phys. B **33**, R1 (2000).
[2] J. Colgan, M. S. Pindzola, and F. Robicheaux, Phys. Rev. Lett. **93**, 053201 (2004); Phys. Rev. A **72**, 022727 (2005).
[3] T. Pattard and J. Burgdörfer, Phys. Rev. A **63**, 020701(R) (2001).
[4] A. Emmanouilidou and J. M. Rost, J. Phys. B **39**, L99 (2006).
[5] R. Wehlitz, M. T. Huang, B. D. DePaola, J. C. Levin, I. A. Sellin, T. Nagata, J. W. Cooper, and Y. Azuma, Phys. Rev. Lett. **81**, 1813 (1998).
[6] R. Wehlitz, T. Pattard, M.-T. Huang, I. A. Sellin, J. Burgdörfer, and Y. Azuma, Phys. Rev. A **61**, 030704 (R)(2000).
[7] I. Taouil, A. Lahmam-Bennani, A. Duguet, and L. Avaldi, Phys. Rev. Lett. **81**, 4600 (1998).
[8] J. Berakdar, A. Lahmam-Bennani, and C. Dal Cappello, Phys. Rep. **374**, 91 (2003).
[9] A. Dorn, G. Sakhelashvili, C. Höhr, A. Kheifets, J. Lower, B. Najjari, C. D. Schröter, R. Moshammer, and J. Ullrich, in *Electron and Photon Ionization and Related Topics (Metz 2002)* edited by L. U. Ancarani (Institute of Physics, Bristol, 2002), pp. 41–51.
[10] M. Dürr, A. Dorn, J. Ullrich, S. P. Cao, A. S. Kheifets, J. R. Götz, and J. S. Briggs (unpublished).
[11] A. W. Malcherek, J. M. Rost, and J. S Briggs, Phys. Rev. A **55**, R3979 (1997).
[12] J. Colgan and M. S. Pindzola, J. Phys. B **39**, 1879 (2006).
[13] A. Emmanouilidou and J. M. Rost, J. Phys. B **39**, 4037 (2006); Phys. Rev. A **75**, 022712 (2007).
[14] P. K. Kabir and E. E. Salpeter, Phys. Rev. **108**, 1256 (1950).
[15] A. Emmanouilidou, T. Schneider, and J. M. Rost, J. Phys. B **36**, 2714 (2003).
[16] R. Abrines and I. C. Percival, Proc. Phys. Soc. London **88**, 861 (1966).
[17] D. J. W. Hardie and R. E. Olson, J. Phys. B **16**, 1983 (1983).
[18] P. Kustaanheimo and E. Stiefel, J. Reine Angew. Math. **218**, 204 (1965).
[19] J. M. Rost, Phys. Rev. Lett. **72**, 1998 (1994).
[20] D. Proulx and R. Shakeshaft, Phys. Rev. A **48**, R875 (1993).
[21] M. Gailitis, J. Phys. B **19**, L697 (1986).